Journal of Magnetic Resonance **157,** 218–222 (2002)
doi:10.1006/jmre.2002.2591

A Rotational Approach to Localized SPAMM 1–1 Tagging

Vasiliki N. Ikonomidou and George D. Sergiadis[1]

Telecommunications Division, Department of Electrical and Computer Engineering, Aristotle University of Thessaloniki, 54124 Thessaloniki, Greece

Received January 22, 2002; revised May 29, 2002; published online August 28, 2002

Magnetic resonance tagging usually relies on controlling the phase dispersion of the transverse magnetization component. Phase dispersion is, however, affected by the inherent phase of selective excitation pulses, thus limiting their combination with tagging sequences to the application of refocusable pulses, as in the localized spatial modulation of magnetization (L-SPAMM) technique. In this study, we examine the effect of selective excitation pulses on a L-SPAMM 1–1 sequence, showing that in the case of two identical pulses the phase component is canceled out, and thus preemphasis and refocus gradients are not needed, allowing us to take advantage of a constant gradient throughout the tagging sequence, and also that one might choose nonrefocusable maximum and minimum phase pulses.

Key Words: **magnetic resonance tagging; localized tagging; SPAMM sequence; selective excitation.**

INTRODUCTION

Noninvasive measurement of tissue motion has always been a challenge in the field of medical imaging. Traditionally, motion is measured as the displacement of a well-defined reference point, such as a marker, over time.

Magnetic resonance tagging is a noninvasive technique for creating such "markers." Measurement of motion is based on the fact that magnetic populations move together with the tissue they belong to. Thus, by locally destroying the longitudinal magnetization component by means of a selective pulse or pulse sequence, one creates a spot that will give no signal in a subsequent imaging sequence. The time between the tagging process and the acquisition of the image data allows for the motion to evolve and deform the tagging pattern (*1*).

In the case of the SPAMM (spatial modulation of magnetization) sequences (*2, 3*), the modulation of the longitudinal magnetization component is achieved by means of a train of alternating nonselective radiofrequency and gradient pulses. In this scheme, the radiofrequency pulses regulate the total magnetization flip angle according to the phase of the transversal component introduced by the gradient pulses. The absence of gradient during the application of the radiofrequency pulse results in the latter being represented as a discrete Dirac function in tagging k-space (*4*). Discreteness results in periodicity in the image space, and thus a uniform grid covering the whole image plane modulates the final image.

However, this is not always desirable, since anatomies are rarely uniform, and in many cases motion is restricted only to specific parts of an image. In order to suit better the needs of nonuniform anatomies, tagging sequences that produce grids with variable separation have recently been proposed (*4, 5*). Since the main tagging pattern is no longer formed by a periodic distribution of M_z, they rely on selective excitation techniques, and result in longer pulse trains.

Chandra and Yang (*6*) presented a simpler approach, aimed at restricting the tagging grid only to a region of interest, thus preserving the anatomical information outside of it. In their approach, the well-known SPAMM and DANTE (*7*) tagging sequences were combined with linear phase selective excitation pulses, whose spectral content defined the region of the image where the tagging grid was to be applied.

The current study elaborates further on the combined application of the SPAMM 1–1 sequence with selective excitation pulses. Its main purpose is to determine the effect of the selective excitation pulse, in terms both of its magnitude—frequency selectivity—and of its phase. Furthermore, it presents a design process based on the analytical results derived from the preceding analysis.

MATHEMATICAL ANALYSIS

Magnetization movement due to a gradient or a radiofrequency pulse may be described as a rotation in the three-dimensional space (*8–10*). By defining $M_{xy} = M_x + iM_y$ the resulting magnetization can be calculated as

$$\begin{bmatrix} M_{xy}^{+} \\ \bar{M}_{xy}^{+} \\ M_z^{+} \end{bmatrix} = \begin{bmatrix} (\bar{\alpha})^2 & -\beta^2 & 2\bar{\alpha}\beta \\ -(\bar{\beta})^2 & \alpha^2 & 2\alpha\bar{\beta} \\ -\bar{\alpha}\bar{\beta} & -\alpha\beta & \alpha\bar{\alpha} - \beta\bar{\beta} \end{bmatrix} \begin{bmatrix} M_{xy}^{-} \\ \bar{M}_{xy}^{-} \\ M_z^{-} \end{bmatrix}, \quad [1]$$

where the $(-)$ and $(+)$ superscripts denote the magnetization before and after the rotation respectively, and α and β are the Cayley–Klein parameters of the rotation.

[1] To whom correspondence should be addressed. Fax: +30 310996312. E-mail: sergiadi@eng.auth.gr.

1090-7807/02 $35.00

It is known (*8–10*) that the Cayley–Klein parameters for a selective excitation pulse may be numerically calculated in the form of two polynomials A and B of order N, that relate to the them as

$$\alpha = z^{N/2}A(z^{-1}) \quad [2]$$

$$\beta = z^{N/2}B(z^{-1}) \quad [3]$$

$$z = \exp(i\gamma Gx\Delta t). \quad [4]$$

γ denotes the gyromagnetic ratio, G the gradient's amplitude, x the population's position along the gradient's axis, and Δt the analysis' time step. z represents the rotation during each time step due to the presence of the gradient.

SPAMM 1–1 tagging is achieved by two identical radiofrequency pulses with a gradient pulse between them. The second pulse transfers the phase induced to the transverse magnetization by the gradient pulse to the longitudinal component, resulting in a sinusoidal modulation of M_z. In the imaging process, this modulation is depicted as brightness variations in the final image.

Use of selective pulses limits the grid to the regions affected by the pulses, since areas where $\beta = 0$ remain unaffected. In the affected regions, the magnetization evolves to

$$M_{xy}^{(1)} = 2\bar{A}BM_0 \quad [5]$$

$$M_z^{(1)} = (A\bar{A} - B\bar{B})M_0 \quad [6]$$

after the first rf pulse,

$$M_{xy}^{(1)+} = 2\bar{A}B\exp(-i\gamma GxT)M_0 \quad [7]$$

after the application of the gradient pulse (T being the duration of the gradient pulse and G its amplitude), and finally

$$\begin{aligned} M_z^{(2)} &= -\bar{\alpha}\bar{\beta}M_{xy}^{(1)+} - \alpha\beta\overline{M_{xy}^{(1)+}} + (\alpha\bar{\alpha} - \beta\bar{\beta})M_z^{(1)} \\ &= -2\mathrm{Re}\left[\bar{\alpha}\bar{\beta}M_{xy}^{(1)+}\right] + (|A|^2 - |B|^2)M_z^{(1)} \\ &= -4\,|A|^2\,|B|^2\,M_0\,\mathrm{Re}[\exp(-i\gamma GxT - 2i\arg(A))z^{-N}] \\ &\quad + (|A|^2 - |B|^2)^2M_0 \\ &= -4\,|A|^2\,|B|^2\,M_0\,\cos[\gamma Gx\,(N\Delta t + T) + 2\arg(A)] \\ &\quad + (|A|^2 - |B|^2)^2M_0. \end{aligned} \quad [8]$$

In the habitual case of $\pi/2$ tagging, the tagging sequence consists of two $\pi/4$ pulses. These are designed by choosing $|B|$ to have a target value of $\sin(\pi/8)$ in its passbands, which define the regions where the grid is active, and zero in the stopbands. Filter A is chosen as the minimum phase filter that satisfies the constrain $|A|^2 + |B|^2 = 1$. By substituting the target values for $|B|$ given above, $|A|$ will vary from 0.924 in the passbands to 1 in the stopbands. Due to the choice of A as a minimum phase filter, its phase will form a Hilbert transform pair with $\ln|A|$. The logarithm function, due to the large mean value of the modulus as compared to its variation, suppresses the range of values for $\arg(A)$, that will, due to the nature of the Hilbert transform, be close to zero in the flat regions of A. Actual values depend on the regions and the flip angle chosen. The phase of A will gain its maximal values in the transition regions of the filter, that, however, correspond to "don't care" regions. Thus, dependence on the $2\arg(A)$ factor, that can lead to grid line displacement and deformation, is minimal in the regions where we are interested in producing a tagging pattern. In fact, its values can be considered to be negligible when compared to the first term of the cosine in Eq. [8].

The above analysis shows that the actual pulse phase, described in usual selective pulse design by filter B does not affect the tagging process as long as the two applied pulses are of equal shape. Thus, one may choose nonrefocusable pulses, like minimum or maximum phase ones, that relatively ease design constraints. Furthermore, no preemphasis or refocus gradient is needed. In fact, the gradient may be kept constant throughout the tagging sequence.

Substituting $|A| = \cos\pi/8$ and $|B| = \sin\pi/8$ for the regions of interest and $|A| = 1$ and $|B| = 0$ for the regions we do not want to be modulated, values that result in a $\pi/4$ pulse in the modulated regions and a zero flip angle elsewhere, and assuming constant gradient throughout the tagging sequence, we get (T_p being the duration of each radiofrequency pulse):

$$M_z^{(2)} \cong \begin{cases} (-\sin^2(\pi/4)\cos[\gamma Gx(T + T_p)] + \cos^2(\pi/4))M_0 & \text{ROI} \\ M_0 & \text{outside.} \end{cases} \quad [9]$$

Equation [9] shows that if the radiofrequency pulses are of sufficient duration, one may not need the separate gradient pulse that in our sequence is the time interval with only gradient application between the radiofrequency pulses. Thus, by expanding the RF pulses in order to cover the whole time interval needed to achieve the desired spacing of the tagging grid, one may come up with a tagging "sequence" consisting of a single radiofrequency pulse.

METHODS

The design process starts by determining the characteristics of an original uniform grid, as in the usual SPAMM 1–1 sequence. From Eq. [9] it follows that the tag separation is defined by $\gamma Gx(T + T_p) = 2\pi$.

Having defined the original uniform grid, one needs to decide which regions are to be kept in the final image. Thus, the next step is to design filter B as a multiband finite impulse response (FIR) filter with passbands in the regions one wants to preserve the tagging lines and stopbands in the regions one wants to keep intact. The filter may be designed by means of any FIR design algorithm, as the Parks–McClellan algorithm (*11*).

The order of the filter B can be calculated from the duration of the pulse and the distance among the selection axis its frequency

response should cover. In general, the latter should be at least equal to or larger than the corresponding image dimensions. This is in order to avoid passbands near the π value of the filter's frequency axis: it is known that the hard pulse approximation is based on the rotation during a Δt period being small enough in order to be modeled as two successive rotations, and values of the order of π might lead to approximation errors. Furthermore, many D/A converters use a zero-order hold approximation in order to implement the radiofrequency envelope. This means that the actual pulse exhibits constant amplitude for periods of Δt. Fourier transform of such a waveform indicates that this may lead to a periodic repetition of the filter's envelope.

The resulting tagging grid profile is calculated as the multiplication of the "envelope" defined by the selective pulse's profile and the comb-like function that defines the original uniform tagging grid. Thus, design constraints on filter B may be eased by taking advantage of the space between the lines of the original grid in order to make larger don't care regions.

The filter B is then used as input to the Shinnar–Le Roux algorithm (*8–10*) in order to design a maximum phase pulse. This is preferred since maximum phase pulses are faster than the equivalent linear phase ones, rephasing is not needed and the maximum phase is transferred in the form of dispersion to the transverse magnetization component at the end of the tagging sequence, thus enhancing the effect of the final spoiler pulse.

RESULTS

As an example, we will demonstrate an L-SPAMM sequence with a multiband pattern.

The pattern is based on an original uniform grid of 33 lines, from which we want to preserve the lines 8, 9, 13, 14, 15, 19, 20, 21, 25, and 26, while keeping the rest of the image intact.

By setting the duration of the gradient pulse between the radiofrequency pulses equal to zero, the number of points we need for the filter equals the number of the tagging lines minus 1, thus 32. Thus, a 62nd order linear phase filter is designed, that is subsequently transformed into a 31st order minimum phase one (*12*). For the filter specifications, since the regions we want to preserve are symmetric around the central point (tagging line 17), we need a multiband filter with two passbands, one covering the lines 19–21 and the second covering the lines 25–26. The intervals between the tagging lines 18–19, 21–22, 24–25, and 26–27 may be used as don't care regions. In order to keep the ripple in the filter's stopbands low, one may choose a greater weight for it: in our example, we used a weight relationship 2 : 1 between stopbands and passbands.

After obtaining a suitable minimum phase filter, a corresponding maximum phase pulse with a $\pi/4$ flip angle is designed by means of the Shinnar–Le Roux algorithm. The tagging sequence consists of two subsequent applications of the resulting pulse, while holding the gradient constant throughout the sequence. Excitation shape is shown in Fig. 1. The resulting tagging pulse's duration was 2.24 ms. In order to calculate tagging sequence duration, one should add the gradient's rise and fall time, yielding in our system a total time of 3.57 ms, which is however dependent both on system characteristics and on the gradient amplitude used. The final spoiler pulse in the slice selection gradient direction is implemented by the rise area of the selection gradient, and thus is not taken into account when calculating sequence duration.

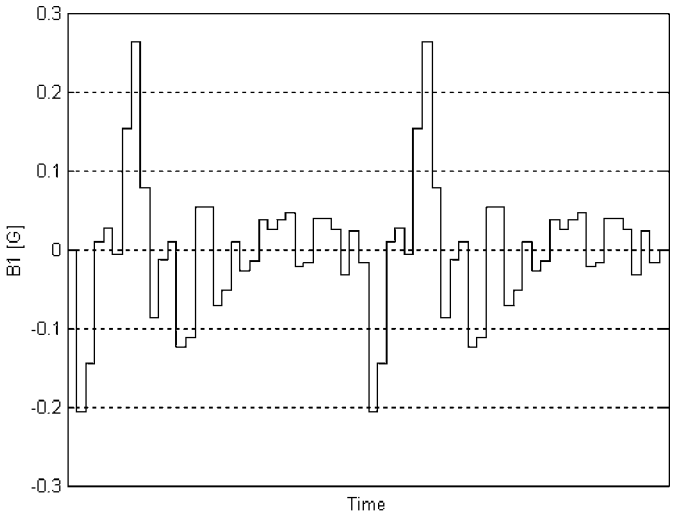

FIG. 1. Excitation pulse shape.

The resulting longitudinal magnetization as obtained from numerical simulation on 2048 discrete magnetization populations is shown, together with the $(1 - |B|^2)$ envelope in Fig. 2. This compares to an experimental profile of an oil phantom shown in Fig. 3. The low values at both sides of the profile are due to the shape of the phantom and indicate noise level. Deviations from the expected profile are due to field inhomogenity, errors

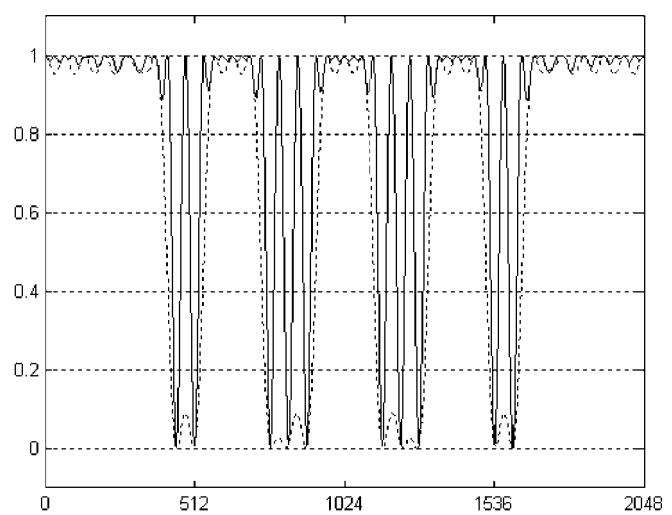

FIG. 2. Simulation results showing predicted envelope (dashed line) and tagging lines (solid line).

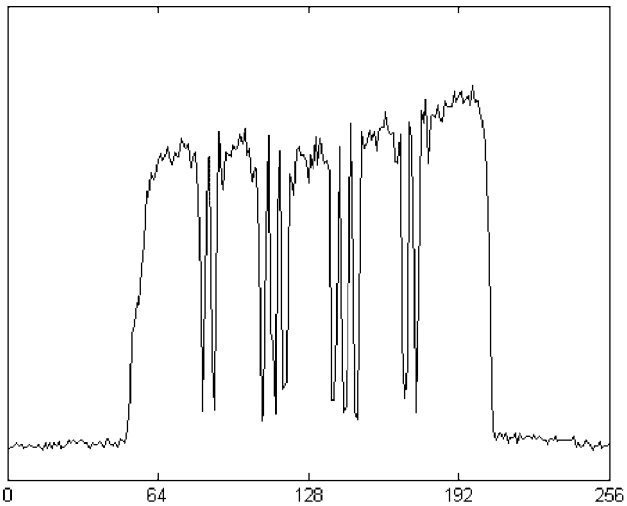

FIG. 3. Experimental tagging profile produced using the pulse of Fig. 1.

in the estimation of the actual flip angle, and integration of the magnetization component through the voxel volume.

The actual image of the oil phantom can be seen in Fig. 4. In the image we see that tagging line quality and contrast are comparable to that of the conventional SPAMM 1–1 method.

Figure 5 shows the results of a similar sequence, preserving tagging lines 2, 3, 6, 7, 8, 14, 15, 16, 19, and 20 out of a 21-line pattern. In the image, one can clearly distinguish a fading of the tagging lines on the sides of the image and the beginning of a second repetition of the grid, both due to the zero-order hold approximation utilized by the D/A converters in order to produce the pulse's envelope. Both grid degradation and the repetition can be avoided using a smaller time step, which in turn would introduce a larger original pattern and a higher order filter for pulse description.

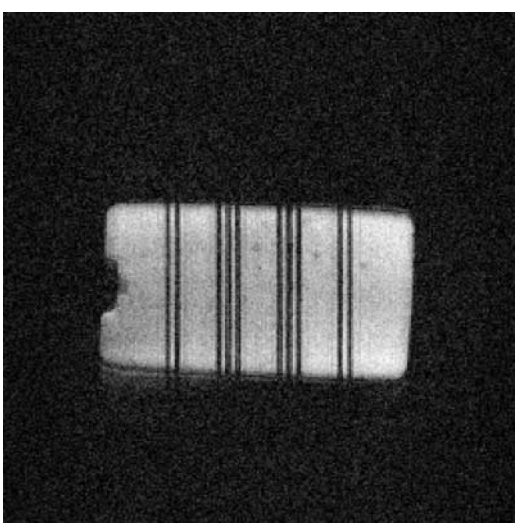

FIG. 4. Actual image of an oil phantom (image taken on a 0.12 T magnet).

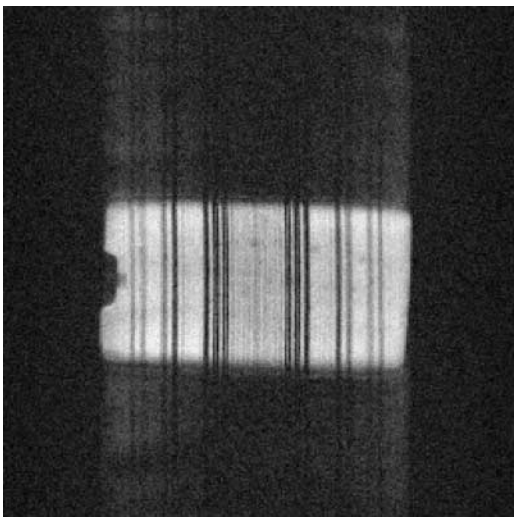

FIG. 5. Image of an oil phantom, with the frequency axis of the filter B accounting for less than the image width. One can note the beginning of a second repetition of the tagging grid at the right side of the phantom and the fading of the tagging lines on the sides of the image, artifacts produced by the zero-order hold approximation used for producing the rf pulse.

DISCUSSION

Localized SPAMM offers an alternative to the usual SPAMM technique, suitable for applications where the motion to be studied is limited to specific areas of the image. In such cases, one can restrict the tagging grid only to the area of the motion, and keep the rest of the image intact, in order to preserve anatomical information.

We have presented a mathematical analysis of the L-SPAMM 1–1 sequence, based on rotation operators, that not only allows estimation of the envelope imposed on the tagging grid, but also gives insight on what happens to the phase distribution as it is affected both by the gradient and by the selective pulses. The result of the analysis was that, provided the two pulses are of the same shape, their effects on the phase distribution cancel out.

This has two distinct effects on the pulse sequence. First, no preemphasis or refocus gradient is needed before or after the radiofrequency pulse, and thus we can have a SPAMM sequence without the gradient pulses proposed in [6]. In fact, the gradient amplitude can be kept constant throughout the tagging sequence. Second, since the sequence is no longer based on the pulse being refocusable, one may choose nonrefocusable pulses like minimum and maximum phase ones. This eases constraints on filter design and allows faster sequences.

Implementation cost lies in software and user interaction. Software is based on fast and robust algorithms, like the Parks–McClellan FIR filter design algorithm and the Shinnar–Le Roux pulse design algorithm. User interaction is used in order to specify the tagging areas.

The technique is readily expandable to two dimensions, by employing the tagging sequence twice, once for each of the axes

of interest. The regions selected during tagging in each axis are independent from each other, and thus complex patterns can also be formed.

REFERENCES

1. E. A. Zerhouni, D. M. Parish, W. J. Rogers, A. Yang, and E. P. Shapiro, Human heart: Tagging with MR imaging—A method noninvasive assessment of myocardial motion, *Radiology* **169,** 59–63 (1988).
2. L. Axel and L. Dougherty, MR imaging of motion with spatial modulation of magnetization, *Radiology* **171,** 841–845 (1989).
3. L. Axel and L. Dougherty, Heart wall motion: Improved method of spatial modulation of magnetization for MR imaging, *Radiology* **172,** 349–350 (1989).
4. W. S. Kerwin and J. L. Prince, A *k*-space analysis of MR tagging, *J. Magn. Reson.* **142,** 313–322 (2000), doi:10.1006/jmre.1999.1946.
5. E. R. McVeigh and B. D. Bolster, Jr., Improved sampling of myocardial motion with variable separation tagging, *Magn. Reson. Med.* **39,** 657–661 (1998).
6. S. Chandra and Y. Yang, Simulations and demonstrations of localized tagging experiments, *J. Magn. Reson. B* **111,** 285–288 (1996), doi:10.1006/jmrb.1996.0095.
7. T. J. Mosher and M. B. Smith, A DANTE tagging sequence for the evaluation of translational sample motion, *Magn. Reson. Med.* **15,** 334–339 (1990).
8. P. Le Roux, Exact synthesis of radiofrequency waveforms, Abstracts of the Society of Magnetic Resonance in Medicine, 7th Annual Meeting, p. 1048, 1988.
9. J. Pauly, P. Le Roux, D. Nishimura, and D. Macovski, Parameter relations for the Shinnar–Le Roux selective excitation pulse design algorithm, *IEEE Trans. Med. Imaging* **10,** 53–65 (1991).
10. M. Shinnar, S. Eleff, H. Subramanian, and J. Leigh, The synthesis of pulse sequences yielding arbitrary magnetization vectors, *Magn. Reson. Med.* **12,** 74–80 (1989).
11. A. Antoniou, "Digital Filters: Analysis, Design and Applications," 2nd ed., McGraw-Hill (1993).
12. N. Damera-Venkata, S. R. McCaslin, and B. L. Evans, Design of optimal minimum phase digital FIR filters using discrete Hilbert transforms. *IEEE Trans. Signal Processing* **48,** 1491–1495 (2000).